

The importance of π - π , π -CH and N-CH interactions in the crystal packing of Schiff-base derivatives of *cis,cis*- and *cis,trans*-1,3,5-triaminocyclohexane

Alexandra L. Pickering, Georg Seeber, De-Liang Long and Leroy Cronin*

Received 12th May 2005, Accepted 15th July 2005

First published as an Advance Article on the web 26th July 2005

DOI: 10.1039/b506718a

The crystal structures of *cis,trans*-1,3,5-*tris*-benzaldimino-cyclohexane (*trans*-tbc, **1**), *cis,trans*-1,3,5-*tris*-(pyridine-2-carboxaldimino)-cyclohexane (*trans*-ttop, **2**), *cis,cis*-1,3,5-*tris*-(pyridine-3-carboxaldimino)-cyclohexane (*cis*-mttop, **3**) and *cis,trans*-1,3,5-*tris*-(pyridine-4-carboxaldimino)-cyclohexane (*trans*-pttop, **4**) are reported. The arrangements of the molecules forming the packed arrays are controlled by the interplay of several different weak intermolecular interactions: π - π stacking, C-H \cdots π and C-H \cdots N interactions, and these are in turn related to differences in the stereochemistry around the cyclohexane backbone, as well as the positioning of the pyridyl-nitrogen to determine the overall supramolecular arrangement of these molecules in the solid state.

Introduction

The supramolecular arrangement in molecular crystals is determined by a range of different intermolecular interactions that vary widely in directionality, strength and specificity.¹ As such, the structural importance of such interactions has been a topic of considerable interest in crystal engineering, molecular recognition, supramolecular assemblies, as well as crystal structure prediction and determination.² The role of conventional hydrogen-bonded interactions is broadly accepted,³ and the impact of weaker forces such as C-H \cdots O and C-H \cdots N hydrogen bonds on crystal packing, in particular in the absence of stronger hydrogen bond donors/acceptors, has also been subject to investigation.^{4,5} This has precipitated interest in all weak intermolecular interactions, including π -stacking interactions, whose importance has been reported in many areas of chemistry, biology and material science.⁶ Aromatic rings can interact in different geometrical arrangements, for example face-to-face, edge-to-face and offset,⁷ and have been found to be a useful tool in the manipulation of molecular components in the crystalline state.⁸ Furthermore, the existence of X-H \cdots π interactions (X = C, N, O; π = aromatic system) is important in structures deficient of strong hydrogen-bond acceptors,^{5,9} and play a role in the crystal structures of both small molecules and larger assemblies such as proteins.¹⁰ Studies into X-H \cdots π interactions show that the T-shaped geometry occurs preferentially at short distances ($d_{\text{H}-\pi}$ 3.0 Å), whereas at longer distances interaction takes place between the H-atom and a ring carbon atom ($d_{\text{H}-\pi}$ 4.0 Å).⁹

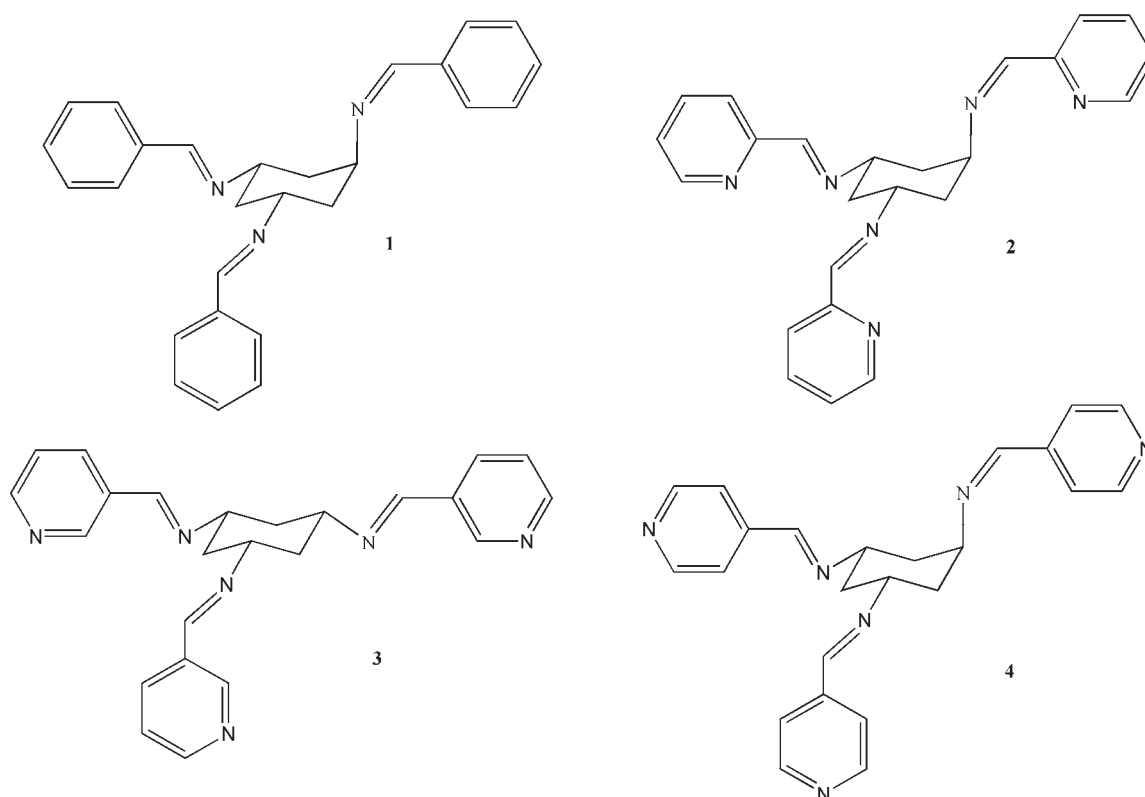
The isomerically related molecules *cis,cis*-1,3,5-triaminocyclohexane (*cis*-tach) and *cis,trans*-1,3,5-triaminocyclohexane (*trans*-tach) have been investigated as ligands for the formation of both discrete¹¹ and extended coordination compounds.¹²

Joseph Black Building, University of Glasgow, Glasgow, UK, G12 8QQ.
E-mail: L.Cronin@chem.gla.ac.uk; Fax: 44 (0)141 330 4888;
Tel: 44 (0)141 330 6661

The derivatisation of these building blocks *via* Schiff-base extensions facilitates the development of the framework in terms of increased numbers of coordinating and possibly chelating moieties. Furthermore, despite being rigid, the cyclohexane backbone has a large degree of conformational flexibility (*i.e.*, ability to ring flip) in addition to the rigid aromatic systems, and the *cis*- and *trans*-stereochemical motifs generate a mixture of identical and non-identical substituted arms. Substitution of the primary amino groups by reaction with benzaldehyde or pyridine-*n*-carboxaldehyde (where *n* = 2, 3 or 4) of these two molecules yields a family of aromatic imines (Scheme 1). These molecules are fundamentally rigid, due to the nature of the aromatic groups and the cyclohexane backbone, and contain the potential for forming multiple supramolecular interactions through C-H \cdots N, C-H \cdots π and π \cdots π interactions.

Results and discussion

The structures of *trans*-tbc, **1** *trans*-ttop, **2** *cis*-mttop, **3** *trans*-pttop, **4** have been investigated crystallographically (see Table 1) and herein we compare and contrast these structures in terms of molecular conformation and supramolecular interactions that determine the crystal packing. The molecule *trans*-mttop has also been synthesised but it proved challenging to grow single crystals. For the sake of comparison of the ability of a *meta*-nitrogen to form interactions, we have included the *cis*-isomer in this study. There are two possible motifs that can be adopted by the cyclohexane ring in the energetically favorable chair conformation: the more stable 'non-flipped' conformation (Scheme 2, LHS) and the 'ring-flipped' conformation (Scheme 2, RHS), which has higher energy due to unfavorable di- or triaxial interactions. This energy barrier can be overcome by the formation of favorable interactions, exemplified by the formation of a variety of coordination compounds by the non-substituted core triamines *cis*-tach¹¹ and *trans*-tach.¹² The steric interactions of the



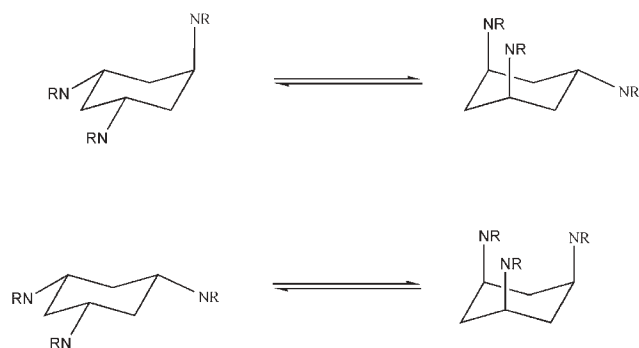
Scheme 1 Depictions of the molecular structures of *cis,trans*-1,3,5-*tris*-benzaldimino-cyclohexane (*trans*-tbc, **1**), *cis,trans*-1,3,5-*tris*-(pyridine-2-carboxaldimino)-cyclohexane (*trans*-ttop, **2**), *cis,cis*-1,3,5-*tris*-(pyridine-3-carboxaldimino)-cyclohexane (*cis*-mttop, **3**) and *cis,trans*-1,3,5-*tris*-(pyridine-4-carboxaldimino)-cyclohexane (*trans*-pttop, **4**)

pyridyl substituents in the ring-flipped conformation, however, make the ring-flipped conformer yet more unfavorable. The difference in the stereochemistry inherited from the

triaminocyclohexane precursor, as well as the positioning of the pyridyl nitrogen in compounds **2–4**, is reflected in the formation of different packing motifs facilitated by the ability

Table 1 Crystallographic data for **1**, **2**, **3** and **4**

Structure	<i>trans</i> -tbc, 1	<i>trans</i> -ttop, 2	<i>cis</i> -mttop, 3	<i>trans</i> -pttop, 4
Empirical formula	C ₂₇ H ₂₇ N ₃	C ₂₄ H ₂₄ N ₆	C ₂₅ H ₂₅ Cl ₃ N ₆	C ₂₄ H ₂₄ N ₆
<i>M</i>	393.52	396.49	515.86	396.49
Crystal system	Monoclinic	Monoclinic	Trigonal	Triclinic
Space group	<i>I</i> 2/ <i>a</i>	<i>P</i> 2 ₁ / <i>n</i>	<i>P</i> $\bar{3}$	<i>P</i> $\bar{1}$
<i>a</i> /Å	18.1262(2)	10.1277(3)	12.6138(7)	6.3273(3)
<i>b</i> /Å	10.4041(1)	19.5020(9)	12.6138(7)	9.5865(5)
<i>c</i> /Å	25.3348(4)	11.3284(5)	9.7434(8)	17.9474(8)
α /°	90	90	90	88.359(3)
β /°	105.974(1)	100.439(2)	90	81.561(3)
γ /°	90	90	120	89.492(3)
<i>V</i> /Å ³	4593.32(14)	2200.44(15)	1342.6(2)	1076.39(9)
<i>Z</i>	8	4	2	2
<i>D</i> /Mg m ³	0.01138	0.01197	0.01276	0.01223
μ /mm ⁻¹	0.516	0.074	0.366	0.076
θ Range/°	3.63 to 59.98	2.09 to 26.00	2.09 to 24.99	2.13 to 25.40
Range of <i>hkl</i>	−20 ≤ <i>h</i> ≤ 20 −9 ≤ <i>k</i> ≤ 11 −27 ≤ <i>l</i> ≤ 28	−12 ≤ <i>h</i> ≤ 12 0 ≤ <i>k</i> ≤ 24 0 ≤ <i>l</i> ≤ 13	−14 ≤ <i>h</i> ≤ 0 0 ≤ <i>k</i> ≤ 14 0 ≤ <i>l</i> ≤ 11	−7 ≤ <i>h</i> ≤ 7 −11 ≤ <i>k</i> ≤ 11 0 ≤ <i>l</i> ≤ 21
<i>F</i> (100)	1680	840	536	420
Parameters	272	271	124	271
Temperature/K	293(2)	150(2)	150(2)	150(2)
Reflections collected	7826	12819	4281	3949
<i>R</i> _{int}	0.0469	0.0457	0.0457	—
Unique reflections	3306	4305	1576	3949
<i>R</i> ₁ [<i>I</i> > 2σ(<i>I</i>)]	0.0715	0.0447	0.0541	0.0462
<i>wR</i> ₂ (all data)	0.1927	0.1016	0.1413	0.1069



Scheme 2 Schematic representation of the two possible conformers of the cyclohexane chair conformation showing low-energy ‘non-flipped’ (LHS) and high-energy ‘ring-flipped’ (RHS).

to form weak interactions involving both the aromatic π -system and the constitute nitrogen atoms.

CCDC reference numbers 271673–271676. See <http://dx.doi.org/10.1039/b506718a> for crystallographic data in CIF or other electronic format.

Framework **1**, *cis,trans*-1,3,5-*tris*-benzaldimino-cyclohexane (*trans*-tbc) has three benzyl substituted imino arms that inherit the *cis,trans*-stereochemistry of the original triamine. Each imine moiety adopts the sterically favoured *E*-conformation with expected bond length [$d_{C=N} = 1.258(2)$ Å]. In the crystal structure, the cyclohexane backbone is found in the energetically most favorable bis-equatorial mono-axial ring conformation, where the phenyl ring in the axial position is nearly perpendicular to the two phenyl rings in equatorial position with an angle of $82.7(1)^\circ$ between the aromatic planes. The equatorial phenyl substituents are twisted by $28.4(1)^\circ$ from coplanarity. The packing motif is dominated by geometrically offset π -stacked interactions between axial phenyl substituents ($d_{\pi-\pi} = 3.4$ Å) and CH– π interactions between equatorial

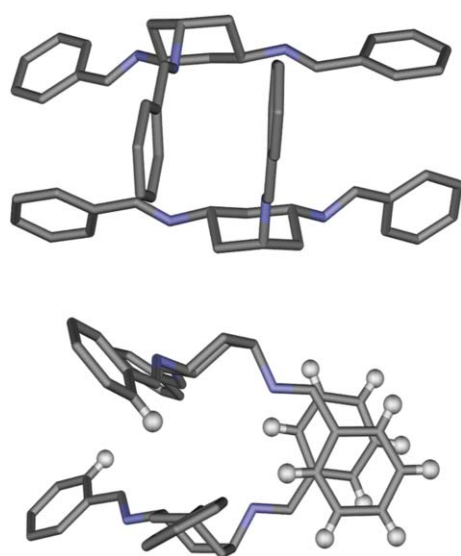


Fig. 1 Dimer of **1**: RHS: representation highlighting π -stacking (3.6 Å) and CH– π (3.0 Å) interactions (with relevant hydrogen atoms shown as white spheres); and LHS: stick representation showing molecular dimer (hydrogens omitted).

phenyl substituents [$d_{H-\pi(\text{centroid})} = 3.2$ Å], which form weakly associated dimers of two *trans*-tbc molecules (Fig. 1).

Additional CH– π interactions between equatorial–equatorial ($d_{H-\pi} = 2.8$ Å) and equatorial–axial ($d_{H-\pi} = 3.0$ Å) phenyl groups connect the dimers into chains along the crystallographic *c*-axis (Fig. 2), which form 2-D layers within the crystallographic *bc*-plane. The layers are arranged in ABABAB fashion along the *a*-axis.

The framework, *cis,trans*-1,3,5-*tris*-(pyridine-2-carboxal-dimino)-cyclohexane (*trans*-ttop, **2**) has three heterocyclic substituents, with each aromatic nitrogen in the *ortho*-position. The crystal structure shows that **2** has adopted the lowest energy conformer to minimise the unfavorable 1,3-diaxial interactions by positioning one substituted arm in axial position and two arms in equatorial positions. The aromatic nitrogen is arranged *anti* with respect to the imine nitrogen, most probably due to the interplay of electronic and crystal packing forces [imine nitrogen ($d_{C=N} = 1.2645(18)$ – $1.2673(19)$ Å)]. In the crystal packing array, layers within the crystallographic *ac*-plane are facilitated by

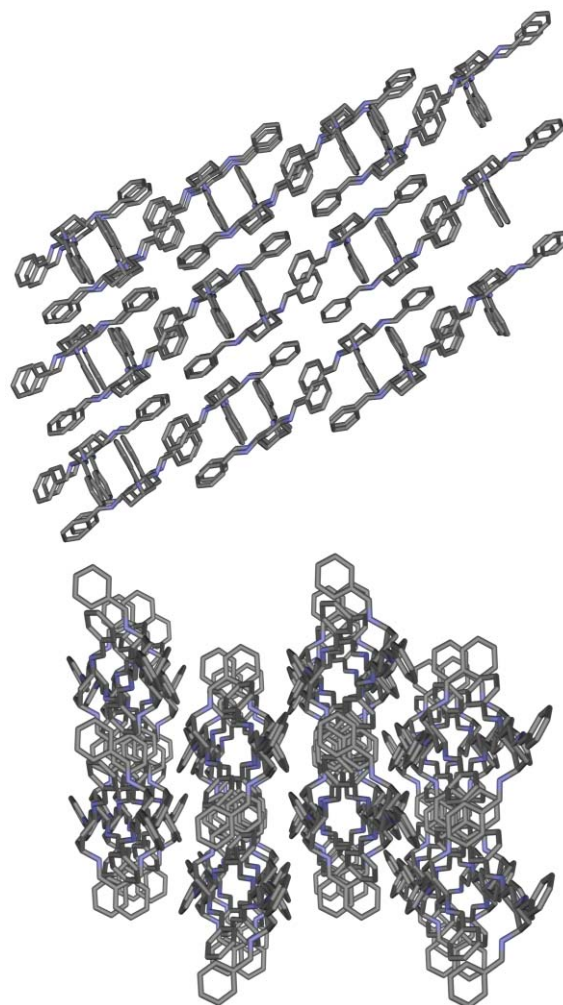


Fig. 2 View of **1** down the crystallographic *b*-axis (RHS) showing chains formed by CH– π interactions [$d_{H-\pi(\text{eq-eq})} = 2.8$ Å, $d_{H-\pi(\text{eq-ax})} = 3.0$ Å] and down the crystallographic *c*-axis (LHS) showing the 2-D layers of weakly interacting molecules. Click here for a rotatable 3-D view of Fig. 2.

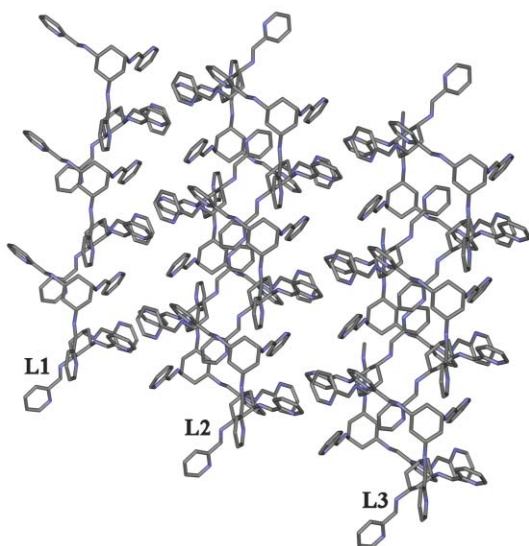


Fig. 3 View of **2** along the crystallographic *b*-axis showing layers of interacting *trans*-ttop ligands within the crystallographic *ac*-plane (L = layer; inter-layer distance = 8.04 Å). Click here for a rotatable 3-D view of Fig. 3.

trans-ttop molecules interlocking through edge-to-edge aromatic–aromatic interactions and C–H...N hydrogen-bonded interactions (Fig. 3).

Each of the three imine ‘arms’ attached to the cyclohexane core interacts with adjacent molecules *via* a slightly different combination of interactions:

(i) The *trans*-axial arm (dark red in Fig. 4) interacts with two *cis*-equatorial arms of two other molecules of **2** forming

CH...N hydrogen-bonded interactions with the imine nitrogen [$N_{(\text{imine})}\cdots\text{CH}_{(\text{aromatic})} = 2.572(8) \text{ \AA}$] with the first and $\pi_{\text{aromatic}}\cdots\pi_{\text{imine}}$ interactions between the imine moiety and an adjacent aromatic ring of the second molecule of **2** [$\pi\cdots\pi = 3.398(4) \text{ \AA}$].

(ii) A *cis*-equatorial arm (blue in Fig. 4) interacts with *trans* and *cis* arm from two different molecules of **2** through a CH hydrogen-bonded interactions with the imine carbon [$N_{(\text{imine})}\cdots\text{CH}_{(\text{aromatic})} = 2.572(8) \text{ \AA}$] and a C–H... π interaction [$\text{C–H}\cdots\pi = 2.656(9) \text{ \AA}$].

(iii) The second *cis*-equatorial arm (yellow in Fig. 4) interacts with another molecule of **2** through a C–H... π interaction [$\text{C–H}\cdots\pi = 2.656(9) \text{ \AA}$].

The framework, *cis,cis*-1,3,5-*tris*(pyridine-3-carboxaldimino)-cyclohexane (*cis*-mttop, **3**) has three crystallographically identical *meta*-pyridyl substituted groups (this symmetry is imposed crystallographically). The crystal structure shows each *cis* arm to be in the energetically favorable equatorial position, with the aromatic nitrogen positioned *anti* with respect to the imine nitrogen [$d_{\text{C=N}} = 1.267(3) \text{ \AA}$]. The ligands pack in isolated layers within the crystallographic *ab*-plane (Fig. 5).

Interestingly, the building blocks do not pack so as to optimise π – π stacking interactions between aromatic systems, but rather position the *meta*-pyridyl groups interstitially between parallel arms of two different *cis*-mttop molecules so as to facilitate C–H...N hydrogen-bonded interactions *via* the aromatic nitrogen atom [$\text{C}_{(\text{imine})}\text{–H}\cdots\text{N} = 3.593(3) \text{ \AA}$]. This forms channels along the crystallographic *c*-axis (Fig. 6), in which the disordered chloroform solvent molecules lie (in-plane with the isolated layers) without forming hydrogen-bonded interactions with the component building blocks. The

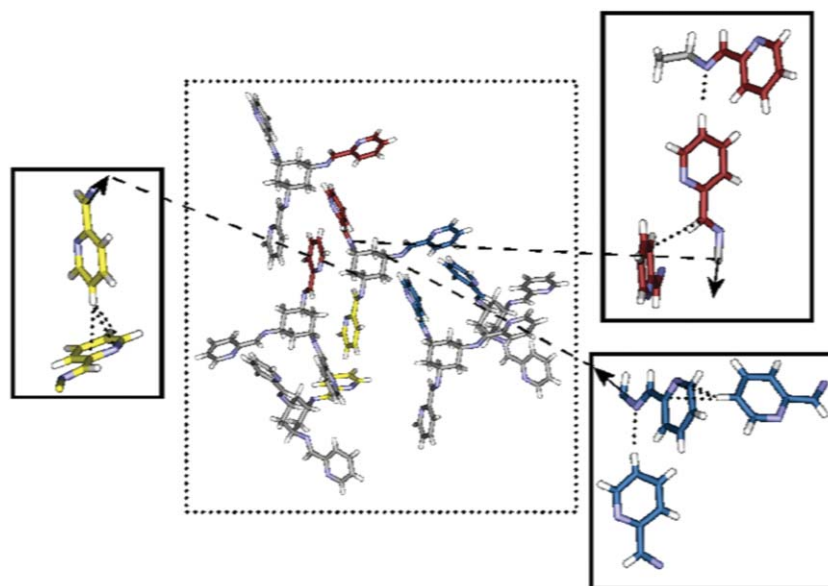


Fig. 4 View of **2** shows how each of the three imine ‘arms’ connected to the cyclohexane core interacts with adjacent molecules of **2** (the arrows depict the arms connected to the core by the dashed line). The *trans* arm (shown in red) takes part in a CH hydrogen-bonded [$N_{(\text{imine})}\text{–H}\cdots\text{CH}_{(\text{aromatic})} = 2.572(8) \text{ \AA}$] and a $\pi_{\text{aromatic}}\cdots\pi_{\text{imine}}$ interaction [$\pi\cdots\pi = 3.398(4) \text{ \AA}$]. The *cis*-equatorial arm shown in blue interacts with a *trans* and *cis* arm from two different molecules of **2** through a CH hydrogen-bonded interactions with the imine carbon [$N_{(\text{imine})}\text{–H}\cdots\text{CH}_{(\text{aromatic})} = 2.572(8) \text{ \AA}$] and a C–H... π interaction [$\text{C–H}\cdots\pi = 2.656(9) \text{ \AA}$]. The second *cis*-equatorial arm shown in yellow interacts with another molecule of **2** through a C–H... π interaction [$\text{C–H}\cdots\pi = 2.656(9) \text{ \AA}$]. The interactions are depicted by the dotted lines.

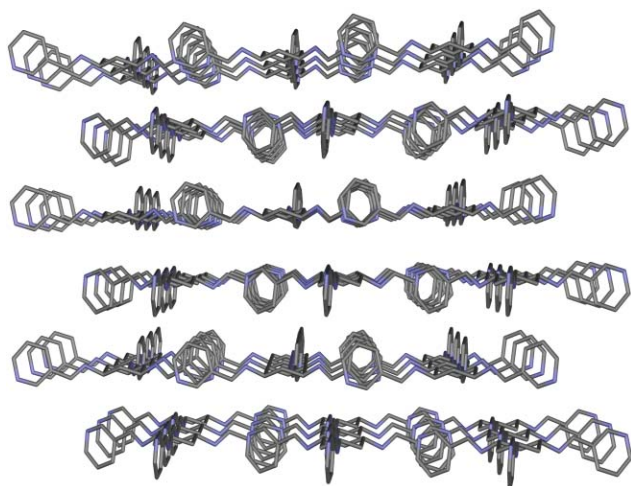


Fig. 5 View of **3** along the crystallographic *a*-axis showing layers of *cis*-mttop ligands within the crystallographic *ab*-plane. Hydrogen atoms and disordered chloroform solvent molecules are omitted for clarity. Click here for a rotatable 3-D view of Fig. 5.

positioning of the pyridyl nitrogen *para* with respect to the imine group in **4**, *cis,trans*-1,3,5-*tris*(pyridine-4-carboxaldimino)-cyclohexane (*trans*-pttop), has a marked effect on the crystal packing array. As is seen in the previous cases, the molecule is found in the non-flipped, bis-equatorial mono-axial chair conformation and forms a 2-D π -stacked network by interaction between crystallographically identical *para*-pyridyl groups. Along the crystallographic *b*-axis, the *trans*-ttop molecules are aligned as a layer divided into rows of two molecules, the difference between which arises from the orientation of the *trans*-axial pyridyl groups along the crystallographic *c*-axis. The *cis*-equatorial pyridyl groups are aligned along the crystallographic *b*-axis (Fig. 7) and form inter-layer

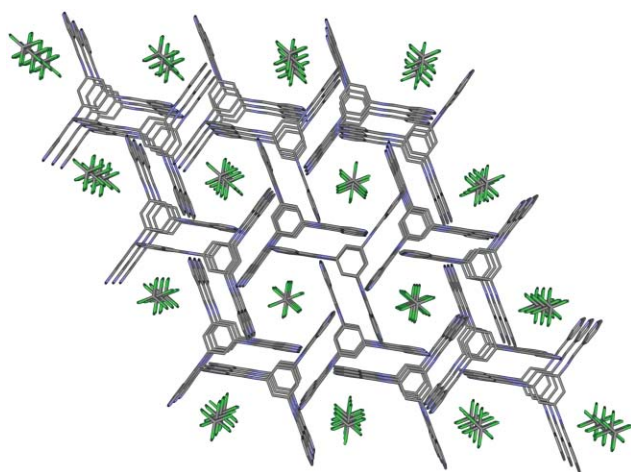


Fig. 6 View of **3** along the crystallographic *c*-axis showing the packing array of *cis*-mttop ligands to form channels that contain disordered chloroform solvent molecules. Carbon atoms are shown as grey sticks, nitrogen atoms in blue and chlorine atoms in green. Hydrogen atoms are omitted for clarity. Click here for a rotatable 3-D view of Fig. 6.

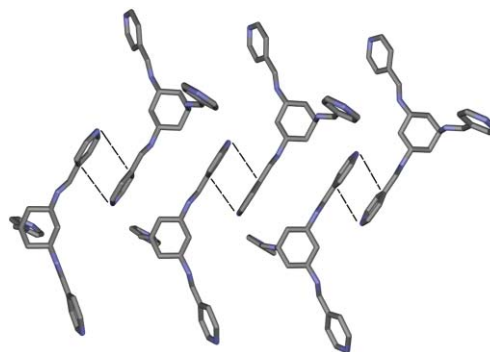


Fig. 7 View of **4** along the crystallographic *a*-axis showing π -stacked interactions between *cis*-equatorial pyridyl groups along the crystallographic *b*-axis (interactions highlighted as dashed lines). Click here for a rotatable 3-D view of Fig. 7.

face-to-face π -stacked interactions with identical pyridyl groups ($d_{\pi-\pi} = 3.7 \text{ \AA}$).

Additional CH- π interactions formed upon insertion of the *trans*-axial arms between the second *cis*-equatorial pyridyl substituents [$d_{\text{H}-\pi(\text{centroid})} = 3.6 \text{ \AA}$] facilitate layers of *trans*-ttop molecules within the crystallographic *bc*-axis (Fig. 8).

Conclusions

The use of the triamino building blocks *cis*- and *trans*-tach in the formation of coordination clusters and arrays is well established,^{11,12} however there is still a lot to gain from study of the uncomplexed frameworks because the weaker interactions dominate and dictate the overall packing in the crystalline state. As such, these investigations have provided valuable insight into the relationship between the various conformational isomers that can be derived from the rigid 1,3,5 tri-substituted cyclohexane backbone. Further, the role of the extended frameworks in transferring conformational information from the cyclohexane backbone to an extended aromatic system has been shown to be of importance in the crystal packing of a family of substituted imines, *via* the

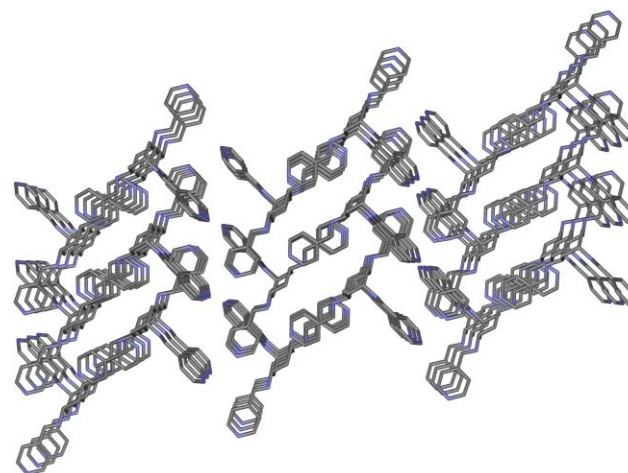


Fig. 8 View along the crystallographic *b*-axis showing layers of interacting molecules. Click here for a rotatable 3-D view of Fig. 8.

formation of supramolecular interactions. Each of the molecules **1–4** packs in a unique array, the formation of which is dependent upon an interplay of weak intermolecular interactions. The absence of a pyridyl nitrogen in *trans*-tbc (**1**) facilitates discrete, offset π stacking interactions that are instrumental in the formation of weakly bound dimers. The addition of a pyridyl nitrogen in *ortho* position has a marked effect on the crystal packing of *trans*-ttop (**2**), which is dominated by the formation of weak C–H \cdots N hydrogen-bonding and the absence of the potential π stacking (aromatic-aromatic) interactions is important in classifying the significance of such C–H \cdots A interactions (where A = weak hydrogen bond acceptor). This is further highlighted in the crystal packing of **3**, whereby layers of *cis*-mttop molecules are arranged by the formation of C–H \cdots N hydrogen-bonded interactions *via* the pyridyl nitrogen in *meta* position. Interestingly, positioning the substituted imine *para* to the pyridyl nitrogen facilitates the formation of a 2-D π -stacked network that also contains C–H \cdots π interactions. The results reported show that small changes in the structural makeup of a family of related building blocks can have a significant impact on their crystal packing. This is due to its dependence on a variety of weak intermolecular interactions, whose directionality and flexibility play an integral role in the crystal engineering of molecular assemblies.

Experimental

cis,trans-1,3,5-tris-Benzaldimino-cyclohexane (*trans*-tbc, **1**)

A solution of *cis,trans*-1,3,5-triaminocyclohexane trihydrochloride (487 mg, 2.04 mmol) and sodium hydroxide (263 mg, 6.58 mmol) in water (15 ml) was stirred for 15 min. Benzaldehyde (58, 706 mg, 6.65 mmol) was added and the resulting mixture ultrasonicated for 4 h. Ether extraction (3 \times 60 ml), drying of the combined organic layers (MgSO₄) and removal of solvent *in vacuo* resulted in an oily residue (2 ml), from which analytically pure **1** crystallised overnight. Addition of hexane (20 ml) and vacuum filtration yielded **1** as a crystalline white solid. Colourless crystals of **1** suitable for single crystal X-ray analysis were obtained by slow evaporation from a concentrated chloroform solution. Yield: 453 mg (1.15 mmol, 56%). ¹H NMR (300 MHz, CDCl₃) δ /ppm 8.41 (s, 2H), 8.38 (s, 1H), 7.82 (2H), 7.73 (4H), 7.45 (3H), 7.40 (6H), 4.11 (tt, 2H, *J* 11.2, 3.5 Hz), 3.95 (t, 1H, *J* 2.8 Hz), 2.10 (m, 3H), 1.96 (bd, 1H, *J* 11.7 Hz), 1.82 (bd, 2H, *J* 11.7 Hz); ¹³C NMR (75 MHz, CDCl₃) δ /ppm 159.74 (CH), 158.84 (CH), 136.56 (C), 130.48 (CH), 128.59 (CH), 128.14 (CH), 65.39 (CH), 63.58 (CH), 41.91 (CH), 40.63 (CH); FTIR (Golden Gate) ν /cm⁻¹ 3063(w), 3032(w), 2932(m), 2862(m), 1636(s), 1582(m), 1450(w), 1381(s), 1296(m), 1211(m), 1134(w), 1065(m), 1026(m), 972(w), 849(m), 756(vs), 687(s); MS (EI+): *m/z* 393; elemental analysis for C₂₇H₂₇N₃, found (exp): % C 82.51 (82.41), H 7.14 (6.92), N 10.67 (10.68).

General procedure for synthesis of pyridyl-based derivatives

A methanolic solution (2 ml) of pyridine-*n*-carboxaldehyde (*n* = 2, 3 or 4, 302 mg, 3.66 mmol) was added to a solution of 1,3,5-triaminocyclohexane (154 mg, 1.19 mmol) and

triethylamine (60 mg, 0.59 mmol) in methanol (30 ml). The mixture was refluxed under nitrogen overnight and the volume reduced to 5 ml. Extraction with dichloromethane (3 \times 20 ml), drying of the combined organic layers (MgSO₄) and removal of solvent *in vacuo* yielded **2–4** as a light-brown solid. Crystals of compounds **2–4** suitable for single crystal X-ray analysis were grown by evaporation of concentrated chloroform solutions.

Analysis for *cis,trans*-1,3,5-tris(pyridine-2-carboxaldimino)-cyclohexane (*trans*-ttop, **2**)

Yield: 82%. ¹H NMR (400 MHz, CDCl₃) δ /ppm 8.56 (1H, 8.53 (2H, *J* 4.5 Hz), 8.40 (s, 2H), 8.38 (s, 1H), 8.02 (1H, *J* 8.0 Hz), 7.90 (2H, *J* 8.0 Hz), 7.68 (1H, *J* 8.0, 7.5 Hz), 7.62 (2H, *J* 8.0, 7.5 Hz), 7.23 (1H, *J* 6.5, 6.0 Hz), 7.12 (2H, *J* 6.5, 6.0 Hz), 4.11 (pt, 2H, *J* 11.3 Hz), 3.97 (bs, 1H), 2.07 (m, 3H), 1.95 (bd, 1H, *J* 12.5 Hz), 1.80 (bd, 2H, *J* 12.5 Hz); ¹³C-NMR (75 MHz, CDCl₃) δ /ppm 159.16 (CH), 158.83 (CH), 153.38 (C), 153.33 (C), 147.95 (CH), 147.84 (CH), 135.00 (CH), 123.20 (CH), 123.10 (CH), 119.99 (CH), 119.75 (CH) 63.48 (CH), 61.68 (CH), 39.90 (CH), 38.68 (CH); FTIR (Golden Gate) ν /cm⁻¹ 3059(w), 2928(m), 2858(m), 1643(s), 1585(s), 1566(s), 1466(s), 1435(s), 1373(m), 1319(w), 1288(w), 1227(w), 1134(m), 1080(m), 1042(m), 1018(w), 991(s), 972(s), 860(s), 772(vs), 741(s), 664(m), 650(m), 617(s), 662(m), 517(s); MS (ES+): *m/z* 419; elemental analysis for C₂₄H₂₄N₆, found (exp): % C 72.53 (72.70), H 6.31 (6.10), N 20.90 (21.20).

Analysis for *cis,cis*-1,3,5-tris(pyridine-3-carboxaldimino)-cyclohexane (*cis*-mttop, **3**)

Yield: 72%. C₂₁H₂₄N₆ (396); C₂₄H₂₄N₆ (396.49): ¹H NMR (CDCl₃): δ /ppm 1.82 (d, 3H, *J* 11.5 Hz), 2.03 (q, 3H, *J* 11.5 Hz), 3.56 (tt, 3H, *J* 3.5, 11.5 Hz), 7.28 (dd, 3H, *J* 4.9, 8.1 Hz), 8.18 (dt, 3H, *J* 1.5, 8.1 Hz), 8.56 (dd, 3H, *J* 1.5, 8.1 Hz), 8.31 (s, 3H), 8.78 (bs, 3H); ¹³C NMR (CDCl₃): δ /ppm 40.234 (CH₂), 65.896 (CH), 123.368 (CH), 142.623 (C), 150.732 (CH), 151.367 (CH), 158.871 (CH), 159.126 (CH); FTIR (Golden Gate): ν /cm⁻¹ 3036 (w), 2952 (m), 1723 (m), 1635 (s), 1597 (s), 1436 (m), 1358 (m), 1307 (s), 1268 (m), 1134 (m), 1060 (m), 978 (s), 916 (w), 813 (s), 630 (m); MS (EI+): *m/z* 396.2; elemental analysis for C₂₄H₂₄N₆(CHCl₃)_{0.5}, found (exp): % C 64.66 (64.59), H 5.47 (5.42), N 18.62 (18.45).

Analysis for *cis,trans*-1,3,5-tris(pyridine-4-carboxaldimino)-cyclohexane (*trans*-pttop, **4**)

Yield: 92%. ¹H NMR (CDCl₃): δ /ppm 1.82 (d, 2H, *J* 12.1 Hz), 1.99 (d, 1H, *J* 11.8 Hz), 2.17 (m, 3H), 4.02 (m, 1H), 4.16 (tt, 2H, *J* 4.1, 11.4 Hz), 7.59 (d, 4H, *J* 5.8 Hz), 7.68 (d, 2H, *J* 5.8 Hz), 8.38 (s, 1H), 8.39 (s, 2H), 8.68 (d, 4H, *J* 5.8 Hz), 8.74 (d, 2H, *J* 5.8); ¹³C NMR (CDCl₃): δ /ppm 40.426 (CH₂), 41.561 (CH₂), 63.828 (CH), 65.838 (CH), 122.307 (CH), 122.423 (CH), 143.413 (C), 143.472 (C), 150.802 (CH), 150.839 (CH), 157.885 (CH), 158.342 (CH); FTIR (KBr): ν /cm⁻¹ 3025 (w), 2925 (m), 2856 (m), 1712 (m), 1641 (s), 1594 (s), 1556 (s), 1457 (m), 1409 (s), 1384 (m), 1313 (s), 1228 (m), 1133 (m), 1060 (m), 989 (s), 869 (m), 811 (s), 730 (s); MS (EI+): 396.2; elemental analysis for C₂₄H₂₄N₆, found (exp): % C: 73.05 (72.70), H: 6.62 (6.10), N: 20.86 (21.19).

Single crystal X-ray diffraction

Suitable single crystals of **1–4** were grown from evaporation of chloroform and mounted onto the end of a thin glass fiber using Fomblin oil. X-ray diffraction intensity data were measured at 150 K on a Nonius Kappa-CCD diffractometer [$\lambda(\text{Mo K}\alpha) = 0.7107 \text{ \AA}$]. Structure solution and refinement for **1–4** was carried out with SHELXS-97¹³ and SHELXL-97¹⁴ via WinGX.¹⁵ Corrections for incident and diffracted beam absorption effects were applied using empirical¹⁶ or numerical methods.¹⁷ Compound **1** crystallized in the space group $I2/a$, compound **2** in $P2_1/n$, compound **3** in $P\bar{3}$ and compound **4** in $P\bar{1}$, as determined by systematic absences in the intensity data, intensity statistics and the successful solution and refinement of the structures. All structures were solved by a combination of direct methods and difference Fourier syntheses and refined against F^2 by the full-matrix least-squares technique. See Table 1 for a summary of the crystallographic parameters.

Acknowledgements

We would like to thank the University of Glasgow and the EPSRC for funding.

References

- 1 J. M. Lehn, *Science*, 1985, **227**, 849; J. W. Steed, *Cryst. Eng. Comm.*, 2003, **5**, 169.
- 2 G. R. Desiraju, *Perspectives in Supramolecular Chemistry Vol. 2*, John Wiley & Sons, Chichester, UK, 1996.
- 3 S. D. Lawrence, T. Jiang and M. Levitt, *Chem. Rev.*, 1995, **95**, 2229; D. C. Sherrington and K. A. Taskinen, *Chem. Soc. Rev.*, 2001, **30**, 83.
- 4 R. Taylor and O. Kennard, *J. Am. Chem. Soc.*, 1982, **104**, 5063; M. Sigalov, A. Vashchenko and V. Khodorkovsky, *J. Org. Chem.*, 2005, **70**, 92.
- 5 G. R. Desiraju, *Science*, 1997, **278**, 404.
- 6 S. K. Burley and G. A. Petsko, *Science*, 1985, **229**, 23; G. B. McGaughey, M. Gagne and A. K. Rappe, *J. Biol. Chem.*, 1998, **273**, 15458; S. Bommarito, N. Peyret and J. SantaLucia, *Nucleic Acids Res.*, 2000, **28**, 1929; P. R. Ashton, R. Ballardini, V. Balzani, I. Baxter, A. Credi, M. C. T. Fyfe, M. T. Gandolfi, M. Gomez-Lopez, M. V. Martinez-Diaz, A. Piersanti, N. Spencer, J. F. Stoddart, M. Venturi, A. J. P. White and D. J. Williams, *J. Am. Chem. Soc.*, 1998, **120**, 11932.
- 7 E. C. Lee, B. H. Hong, J. Y. Lee, J. C. Kim, D. Kim, Y. Kim, P. Tarakeshwar and K. S. Kim, *J. Am. Chem. Soc.*, 2005, **127**, 4530; C. A. Hunter, K. R. Lawson, J. Perkins and C. J. Urch, *J. Chem. Soc., Perkin Trans. 2*, 2001, 651.
- 8 I. Dance, *CrystEngComm*, 2003, **5**, 37, 208.
- 9 G. R. Desiraju and T. Steiner, *The Weak Hydrogen Bond in Structural Chemistry and Biology*, Oxford University Press, Oxford, UK, 1999.
- 10 T. Steiner and G. Koellner, *J. Mol. Biol.*, 2001, **305**, 535; M. Nishio, *CrystEngComm*, 2004, **6**, 27, 130; F. J. Malone, C. M. Murray, M. H. Charlton, R. Docherty and A. J. Lavery, *J. Chem. Soc., Faraday Trans.*, 1997, **93**, 19, 3429; P. Hobza and Z. Havlas, *Chem. Rev.*, 2000, **100**, 4253 and references therein.
- 11 J. Y. Yang, M. P. Shores, J. J. Sokol and J. R. Long, *Inorg. Chem.*, 2003, **42**, 1403; U. Brand and H. Vahrenkamp, *Inorg. Chim. Acta*, 1992, **198**, 663.
- 12 A. L. Pickering, G. Seeber, D.-L. Long and L. Cronin, *Chem. Commun.*, 2004, 136; A. L. Pickering, D.-L. Long and L. Cronin, *Inorg. Chem.*, 2004, **43**, 4953.
- 13 G. M. Sheldrick, *Acta Crystallogr., Sect. A*, 1998, **A46**, 467.
- 14 G. M. Sheldrick, *SHELXL-97, Program for Crystal structure analysis*, University of Göttingen, Germany, 1997.
- 15 L. J. Farrugia, *J. Appl. Crystallogr.*, 1999, **32**, 837.
- 16 R. H. Blessing, *Acta Crstallogr., Sect. A*, 1995, **51**, 33.
- 17 P. Coppens, L. Leiserowitz and D. Rabinovich, *Acta Crystallogr.*, 1965, **18**, 1035.